Polycrystalline solids under nonhydrostatic compression: Determination of strength from x-ray diffraction data

A K Singh
Scientist and Head (retired), Materials Science Division, National Aerospace Laboratories, Bangalore 560 017, India

E-mail: singhnal@yahoo.com

Abstract. A polycrystalline sample compressed in a diamond anvil cell (DAC) without any pressure transmitting medium develops a stress state at the centre of the sample that is axially symmetric about the load axis. The axial stress component is larger than the radial component and the difference *t* between the two is taken as a measure of the compressive strength of the sample material at a confining pressure that equals the mean normal stress. A proper analysis of the diffraction data yields *t*. The data taken with the radial diffraction geometry, wherein the incident x-ray beam is perpendicular to the load axis of the DAC, give reliable estimates of strength. The diffraction data obtained with the conventional geometry, wherein the incident x-ray beam passes parallel to the DAC axis, provide reasonable estimates of strength. However, even in this case, reliable strength data can be obtained by combining the measured pressure-volume data under nonhydrostatic compression and the hydrostat derived from an independent source. The determination of strength from high pressure diffraction data is discussed.

1. Introduction

The diamond anvil cells (DAC) are routinely used to pressurize polycrystalline samples to a few hundred gigapascals (GPa). The x-ray diffraction patterns from the compressed samples give useful information on the pressure-volume relation and phase transitions. The stress state of the sample compressed in a DAC invariably turns nonhydrostatic. The nonhydrostatic stresses have been modelled [1,2] and the equations describing the effect of such stresses on the measured $d_{\mathrm{m}}(hkl)$ have been derived [1,3–8]. The analyses of $d_{\mathrm{m}}(hkl)$ using these equations give information on the volume compression produced by the hydrostatic component of stress, compressive strength and single crystal elastic moduli under high confining pressure. Full range of information can be obtained only when $d_{\mathrm{m}}(hkl)$ are measured with special geometry called radial diffraction. The diffraction patterns recorded with the commonly used geometry, wherein the incident x-ray beam is parallel to the load axis, give limited information. The scope of this paper is limited to the estimation of the compressive strength of the sample from the $d_{\mathrm{m}}(hkl)$ measured under nonhydrostatic compression. The equations required for the analysis and the various diffraction geometries used are discussed. The strengths of a few metals, as derived from diffraction data recorded with different geometries, are presented.

2. Nonhydrostatic stresses and line shift

In the experiments conducted for the determination of strength, the polycrystalline solid is compressed between the anvils without any pressure medium in order to maximize the nonhydrostatic stresses. As the DAC is loaded, the sample is compressed axially and begins to flow radially. At small loads, the

sample slips between the anvil surfaces and friction between the sample-anvil interfaces oppose the outward flow. At higher loads the slippage stops and the sample begins to shear. When the flow of the sample ceases, complex equilibrium stresses are established. One recognizes mean stress over a length scale of the order of 5–10 μm. These stresses are termed macro-stresses. These stresses produce macro-strains that cause diffraction lines to shift. The micro-stresses are related to the second moment about the mean of the stress distribution. These produce micro-strains that cause the diffraction lines to broaden. In this section we consider only the macro-stresses and its effect on the measured $d_{\mathrm{m}}(hkl)$.

In a well aligned DAC the diamond faces are parallel and the incident x-ray beam passes parallel to the load axis at the centre of the anvil face. Noting that the macro-stresses possess axial symmetry about the load axis, the stress state at a small area is given by a stress component σ_{33} along the load direction and two equal components σ_{11} parallel to the anvil face. The nonhydrostatic stress is given by a tensor [1,2],

$$\sigma_{ij} = \begin{vmatrix} \sigma_{11} & 0 & 0 \\ 0 & \sigma_{11} & 0 \\ 0 & 0 & \sigma_{33} \end{vmatrix} = \begin{vmatrix} \sigma_{\mathrm{P}} & 0 & 0 \\ 0 & \sigma_{\mathrm{P}} & 0 \\ 0 & 0 & \sigma_{\mathrm{P}} \end{vmatrix} + \begin{vmatrix} -t/3 & 0 & 0 \\ 0 & -t/3 & 0 \\ 0 & 0 & 2t/3 \end{vmatrix} = \sigma_{\mathrm{P}} + D_{ij} \qquad (1)$$

The σ_{P} is the mean normal stress or equivalent hydrostatic pressure and equals $(\sigma_{11}+\sigma_{11}+\sigma_{33})/3$. D_{ij}, termed deviatoric stress, is a tensor. The term *t*, often termed differential stress, is given by, $t=(\sigma_{33}-\sigma_{11})$. Further, it is suggested [2] that $t \le \sigma_{\mathrm{Y}}$, where σ_{Y} is the yield strength under the confining pressure σ_{P}. The off-diagonal terms in equation (1) vanish only if the diffraction takes place from a small region at the center of the sample. The main factor that causes the off-diagonal terms to appear is the diffracted intensity from the regions of stress gradient that progressively increases with increasing pressure σ_{P}. Thus, the off-diagonal terms are small at low pressure in the experiments with a well-aligned DAC and incident beam setup, and gradually increases with increasing pressure. A complete discussion of this aspect is given elsewhere [9].

The equations describing the effect of D_{ij} on $d_{\mathrm{m}}(hkl)$ for different crystal systems have been derived [3, 6–7]. The following equation is general and valid for all crystal systems with the x-ray beam incident on the sample in an arbitrary direction

$$d_{\mathrm{m}}(hkl) = d_{\mathrm{P}}(hkl)[1+(1-3\cos^2\psi)Q(hkl)] \qquad (2)$$

The term $d_{\mathrm{P}}(hkl)$ denotes the *d*-spacing produced by σ_{P}, and ψ is the angle between the load axis of the DAC and the diffracting plane normal. The term $Q(hkl)$ is given by

$$Q(hkl) = \frac{t}{6}\{\alpha[G_{\mathrm{R}}^{\mathrm{X}}(hkl)]^{-1} + (1-\alpha)[G(\mathrm{V})]^{-1}\} \qquad (3)$$

Here $G_{\mathrm{R}}^{\mathrm{X}}(hkl)$ is the diffraction shear modulus. It represents the shear modulus under the assumption of stress continuity across the grains averaged only over the crystallites that contribute to the diffraction intensity at the point of observation. In a sample with randomly distributed crystallites, it represents single crystal shear modulus. $G(\mathrm{V})$ denotes the shear modulus of the aggregate under the assumption of the strain continuity. The parameter α is a weight factor. In early work its value was assumed to lie between 0.5 and 1. In a recent study [9], it has been shown that for the cubic system, the relevant value of α depends on the elastic anisotropy factor $x = 2(S_{11}-S_{12})/S_{44}$. For $x \ge 1$, $\alpha \le 1$ and for $x \le 1$, $\alpha \ge 1$. For the cubic system,

$$[G_{\mathrm{R}}^{\mathrm{X}}(hkl)]^{-1} = 2[(S_{11}-S_{12}) - 3(S_{11}-S_{12}-S_{44}/2)\Gamma(hkl)] \\ = S_{44}[x - 3(x-1)\Gamma(hkl)] \tag{4.1}$$

$$\Gamma(hkl) = (h^2k^2 + k^2l^2 + l^2h^2)/(h^2+k^2+l^2)^2 \tag{4.2}$$

$$[G(\mathrm{V})]^{-1} = S_{44}[5x/(3x+2)] \tag{4.3}$$

$G_{\mathrm{R}}^{\mathrm{X}}(hkl)$ for all crystal systems are given elsewhere [7]. The expression for *t* can be derived by multiplying both sides of equation (2) by the aggregate shear modulus *G* and expressing *G* as the harmonic mean of *G*(R) and *G*(V), *G*(R) being the aggregate shear modulus under the condition of stress continuity across the grains.

$$[G]^{-1} = \{[G(\mathrm{R})]^{-1} + [G(\mathrm{V})]^{-1}\}/2 \tag{5}$$

Noting that $[G(\mathrm{R})]^{-1} = S_{44}[(2x+3)/5]$, the following expression is obtained for *t*

$$t = 6G\langle Q(hkl)\rangle f(x,\alpha) \tag{5.1}$$

The symbol $\langle Q(hkl)\rangle$ denotes the average of all observed $Q(hkl)$.

$$f(x,\alpha) = A/B \tag{5.2}$$

$$A = \{[(2x+3)/10] + 5x/[2(3x+2)]\} \tag{5.3}$$

$$B = \{\alpha[x - 3(x-1)\langle\Gamma(hkl)\rangle] + 5x(1-\alpha)/(3x+2)\} \tag{5.4}$$

The function $f(x,\alpha)$ has been shown in figure (1) for a wide range of *x* and α. Noting that $\alpha \le 1$ if $x \ge 1$, and $\alpha \ge 1$ if $x \le 1$, it is seen that $f(x,\alpha) \cong 1$ for the elastic anisotropy encountered in practice. An interesting example is that of niobium [10]. The elastic anisotropy *x* of niobium changes from ~0.5 at ambient pressure to ~0.4 at 40 GPa. The α-value decreases from 2.5 to 1.4 over this pressure range. It is shown [10] that $f(x,\alpha) \cong 0.95$ over the entire pressure range.

For the crystal systems of lower symmetry, it is not possible to determine the bounds on α, as it could be done for the cubic system [9], because the anisotropy factor is not defined by a single parameter. For highly anisotropic solids of the hexagonal system such as, beryllium, apatite, beryl, muscovite, cancrinite, and many more, computation of $f(x,\alpha)$ using the single crystal elastic moduli indicates that for $\alpha = 0.5$, it varies between 0.9 and 1.1. For these reasons, $f(x,\alpha) \cong 1$ is assumed to be valid for all the crystal systems. The strength *t* is, therefore, given by

$$t = 6G\langle Q(hkl)\rangle \tag{6}$$

Equation (6) is often misinterpreted as an equation based on shear modulus scaling. It is seen that no such assumption is made in the derivation of equations (5.1) and (6). Further, *G* is conventionally given by the arithmetic mean of *G*(R) and *G*(V). In equation (5), harmonic mean has been used. This was done to maintain uniformity with equation (3). For commonly encountered elastic anisotropy *x*, the two means do not differ significantly.

If the $d_m(hkl)$ can be measured at different ψ, then $Q(hkl)$ can be obtained from equation (2). The radial geometry that permits measurement of $d_m(hkl)$ at different ψ is shown in figure (2a) and (2b). It is seen that equation (6) requires only the aggregate shear modulus *G* as an external input. The aggregate shear modulus *G* at high pressure can be obtained using a finite strain equation of the form

$$G = G_0 y^{5/3}[1 + \tfrac{1}{2}(3K_0G_0^{'}/G_0 - 5)(y^{2/3} - 1)] \tag{6.1}$$

Here, G is the aggregate shear modulus at a pressure σ_P. K_0, G_0 and $G_0^{'}$ are the bulk modulus, shear modulus and its pressure derivative at ambient pressure, respectively. The volume compression V_0/V at a pressure σ_P is denoted by *y*. K_0, G_0 and $G_0^{'}$ are available from the ultrasonic velocity measurements on a single crystal for most solids.

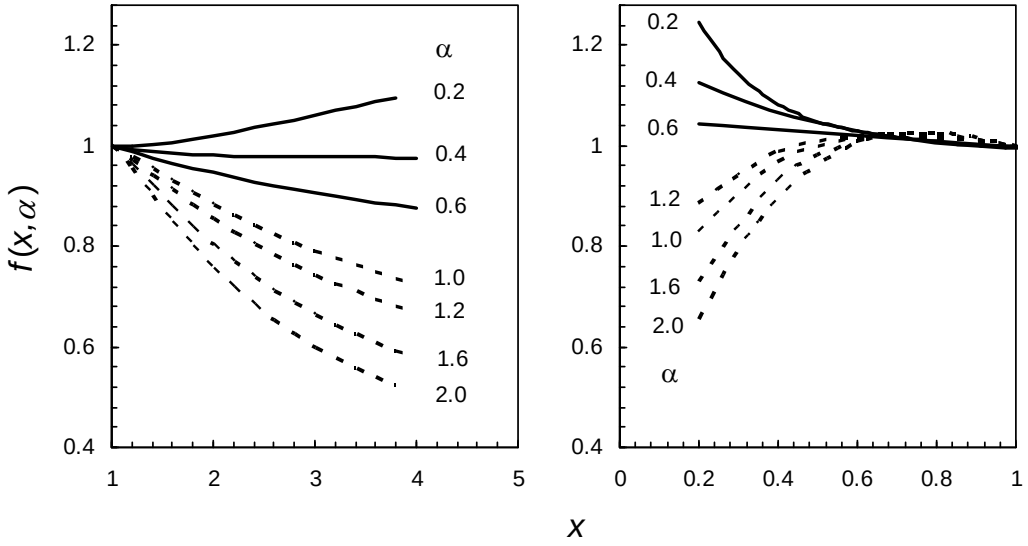

Figure 1. Plot $f(x,\alpha)$ as function of *x* for various α values.

Most investigators use the conventional geometry to record the diffraction data. These data can be used to determine *t*. It was pointed out in an earlier study [11] that, at any pressure, the unit cell volume measured in presence of nonhydrostatic stresses is overestimated. As a result, there is an offset between the hydrostat and the measured equation of state. This offset can be used to estimate *t* by using a relation proposed earlier [4]. This expression is of the form

$$t = \left[\frac{V_m - V_P}{V_P}\right] \frac{2G}{\langle(1 - 3\sin^2\theta)\rangle} \tag{7}$$

The terms V_m and V_P denote the unit cell volumes under nonhydrostatic and hydrostatic pressure, respectively. It is to be noted that, unlike equation (2), this method requires two parameters, *G* and V_P, in addition to the measured V_m.

For the cubic system, equation (2) suggests [12] that a plot of the lattice parameter $a_m(hkl)$, measured in presence of nonhydrostatic stresses, versus $3\Gamma(hkl)(1-3\sin^2\theta)$ is a straight line and *t* is given by

$$t = -3M_1/[\alpha M_0(S_{11} - S_{12} - S_{44}/2)] \quad (8)$$

The terms M_0 and M_1 are the intercept and slope, respectively, on the $3\Gamma(hkl)(1-3\sin^2\theta)$ axis, of the plot. This plot is termed gamma-plot. Equation (8) with $\alpha = 1$ is identical with the result of equation (12) of Singh and Kennedy [1], an equation found so useful in detecting the onset of nonhydrostatic stresses as the pressure of the sample is increased. It is to be noted that this method requires single crystal elastic moduli and their pressure derivatives. Additionally, the parameter α, a parameter with large uncertainty, is also required.

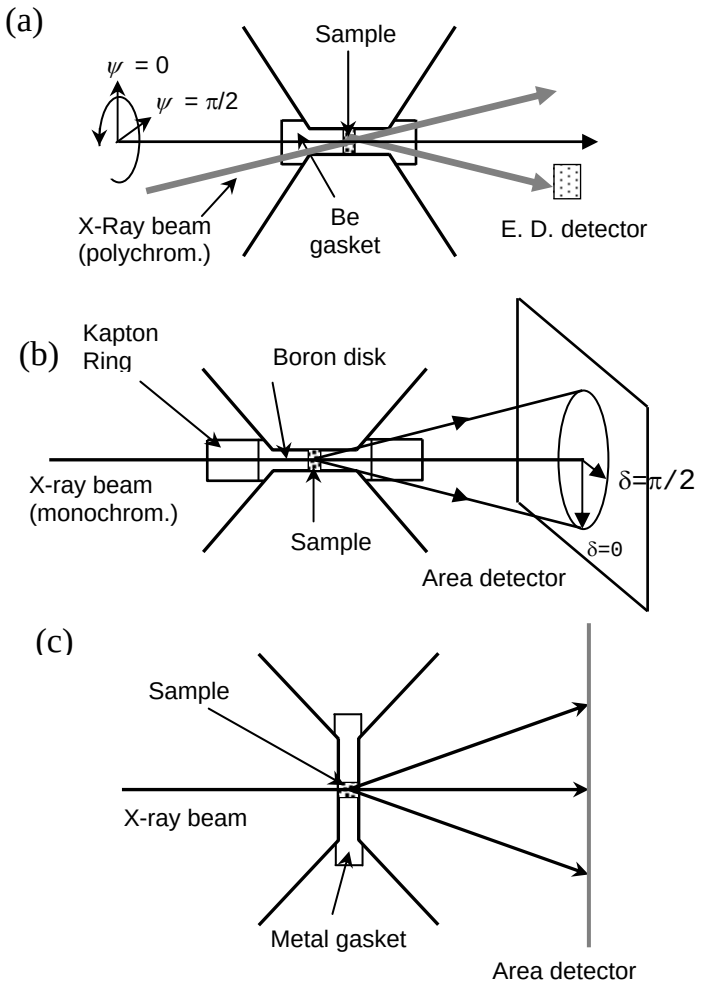

Figure 2. (a) The radial diffraction geometry [13] with accessible ψ-range $0 \le \psi \le 360^\circ$. **(b)** Another version of radial geometry (side diffraction) [14-16] is shown with accessible ψ-range $\theta \le \psi \le 90^\circ$. This range repeats in remaining three quadrants. The angle δ is related to ψ by $\cos\psi = \cos\delta\cos\theta$. **(c)** This figure shows the conventional geometry. Here, $\psi = \pi/2 - \theta$.

3. Some examples

Equation (6) has been used extensively to determine the strength as a function of pressure. A review [17] covers the important stress measurement activities prior to 2007. The review of the entire literature is beyond the scope of this article. However, it is worth mentioning a few interesting studies that have appeared more recently. The estimation of strength of solid argon using radial diffraction data suggests that by 40 GPa, it develops strength that is comparable to that of steel at the same pressure [18]. Helium under high pressure is a solid that retains fluid-like shear property better than any other material and, for this reason, it is used as pressure transmitting medium in experiments with DAC. A study shows that strength of helium is ~2 GPa at 100 GPa [19]. Studies on superhard ceramics such as BC_2N [20] and WB [21] suggest that these solids undergo very high strengthening under compression in a DAC. Among the pure metals, osmium has the highest strength that reaches nearly 10 GPa at 26 GPa [22].

Equation (7) provides an equally reliable method of determining strength under high confining pressures. The strength of rhenium has been examined by this method to 250 GPa [23] and to 120 GPa [24]. Strength of rhenium has also been measured using the radial diffraction data to 37 GPa [25]. A comparison of the results of these studies is given in figure (3). The three sets of data are in good agreement in the overlapping pressure region. This agreement shows the equivalence of equations (6) and (7). One of the shear moduli $(C_{11} - C_{12})$ of stishovite phase of silica decreases under pressure and vanishes at ~50 GPa marking a transition to $CaCl_2$ type structure. The strength across the phase transition has been measured using equation (6) [26] and equation (7) [27]. In this case also the results of the two studies agree well.

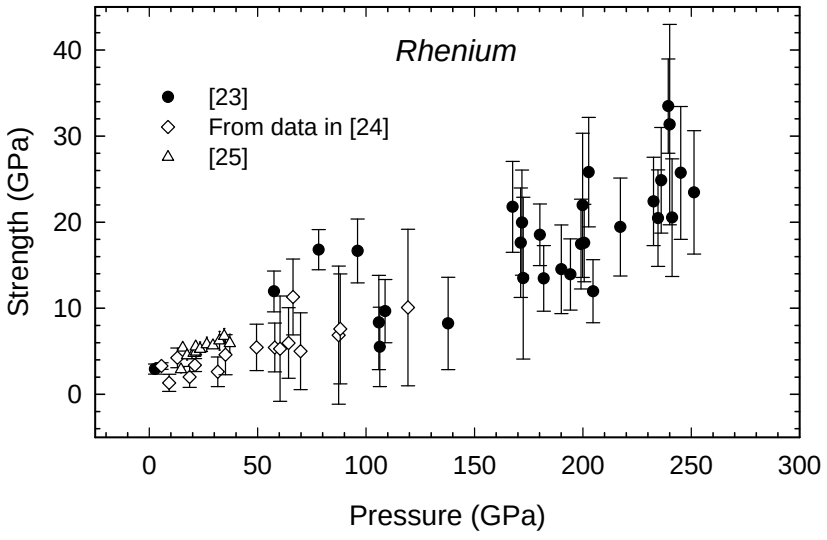

Figure 3. A comparison of strength of rhenium from three different studies.

Equation (8) has been used to determine strength in spite of its drawback that it requires single crystal elastic compliances and α. As an example, the strength of gold, as determined in several studies, are shown in figure (4). The data [28,31] are obtained by using equation (8) while the data [25, 29] are obtained using equation (6). While the agreement among different sets of data is good, the point to be noted is that $\alpha = 0.5$ has been used in [28] whereas $\alpha = 1$ is used in [31], suggesting that at any given pressure, the strength obtained in [28] should be twice that in [31]. The difference between the two sets of data is much less. As observed in [9], $\alpha \leq 1$ because $x > 1$ for gold. The two sets of data [28,31] below 40 GPa can be brought in to good agreement if α between 0.5 and 1 is chosen.

However, same value of α at higher pressure will lead to divergence between the two sets. This would suggest a pressure dependent α, a trend noticed earlier [10]. Further source of differences among the various sets could be the varying degree of purity of the samples used in these studies. However, the large scatter in the data arising from the measurement errors makes it difficult to discuss these factors.

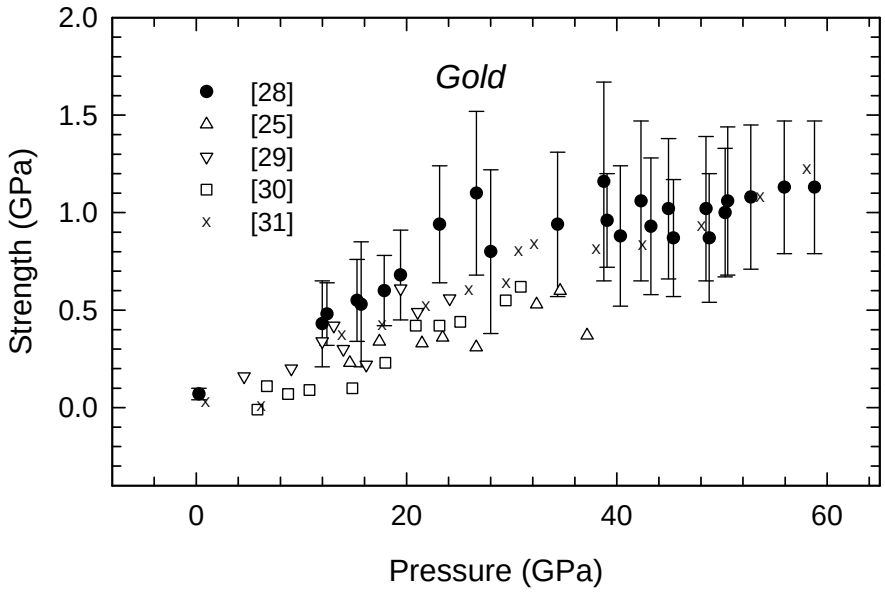

Figure 4. A comparison of strength of gold from different studies.

Table 1. A comparison of tensile strength of a few elements and *t* at 0 GPa from high pressure experiments. Annealed – a. Cold worked – cw.

Element	UTS (GPa) references [32,33]	*t* (GPa) at 0 GPa
Al	0.11 (a)	0.2 [34]
Au	0.125 (a); 0.22 (cw)	0.15 [25,28–31]
Ag	0.17	0.18 [35]
α-Fe	0.3	0.5 [36]
Mo	0.6	0.46 [29]
Pt	0.12–0.17 (a); 0.21–0.24 (cw).	0.21 [37]
Re	1.16 (a); 2.22 (cw)	2.25 [24–26]
W	2.35	2.4 [38]

Table 1 shows that the tensile strength measured in a standard test on bulk specimen are in good agreement with the corresponding values derived from the high pressure measurements. A comment on the pressure dependence of strength from these studies is in order. Under nonhydrostatic compression the sample undergoes plastic deformation (strain or work hardening) and grain size reduction. Both these factors contribute to increase in strength [39–41]. In metals such as rhenium, work hardening is a major factor that contributes to the strength. In brittle materials like ceramics, it is the grain size reduction that accounts for the rapid increase of strength-pressure data. For these reasons, the increase in strength with pressure derived from x-ray data is expected to be higher than that under hydrostatic pressure.

References

[1] Singh A K and Kennedy G C 1974 *J. Appl. Phys.* **45** 4686–91
[2] Ruoff A L 1975 *J. Appl. Phys.* **46** 1389–92
[3] Singh A K 1993 *J. Appl. Phys.* **73** 4278–86. Erratum *J. Appl. Phys.***74** 5920
[4] Singh, A K and Balasingh C 1994 *J. Appl. Phys.* **75** 4956–62
[5] Uchida T, Funamori N and Yagi T 1996 *J. Appl. Phys.* **80** 739–46
[6] Singh A K, Mao H-k, Shu J and Hemley R J 1998 *Phys. Rev. Lett.* **80** 2157–60
[7] Singh A K, Balasingh C, Mao H-k, Hemley R J and Shu J 1998 *J. Appl. Phys.* **83** 7567–75
[8] Singh A K 2004 *J. Phys. Chem. Solids* **65** 1589–96
[9] Singh A K 2009 *J. Appl. Phys.* **106** 043514
[10] Singh A K and Liermann H-P 2011 *J. Appl. Phys.* **109** 113539
[11] Singh A K 1978 *High Temp. High Press.* **10** 641-650
[12] Singh A K and Takemura K 2001 *J. Appl. Phys.* **90** 3269–75
[13] Mao H K and Hemley R J 1996 *High Press. Res.* **14** 257–267
[14] Kinsland G L and Bassett W A 1976 *Rev. Sci. Instrum.* **47** 130–33
[15] Singh, AK 1994 *AIP Conf. Proc.* **309** 1629–32
[16] Merkel S and Yagi T 2005 *Rev. Sci. Instrum.***76** 046109
[17] Duffy T S 2007 *AIP Conf. Proc.* **955** 639–44.
[18] Mao K-k, Badro J, Shu J, Hemley R J and Singh A K 2006 *J. Phys.: Condens. Matter* **18** S963-68
[19] Singh A K 2012 *J. Phys.: Conf. Ser.* **377** 012007
[20] Dong H, He D, Duffy T S and Zhao Y 2009 *Phys. Rev.* B **79** 014105
[21] Dong H, Dorfman S M, Chen Y, Wang H, Wang J, J Qin, He D and Duffy T S 2012 *J. Appl. Phys.***111** 123514
[22] Weinberger M B, Tolbert S H and Kavner A 2008 *Phys. Rev. Lett.* **100** 045506
[23] Singh A K, Hu J, Shu J, Mao H-k and Hemley R J 2012 *J. Phys.: Conf. Ser.* **377** 012008
[24] Jeanloz R, Godwal B K and Meade C 1991 *Nature* **349** 687–9
[25] Duffy T S, Shen G, Heinz D L, Ma Y, Shu J, Mao H K, Hemley R J and Singh, A K 1999, *Phys. Rev.* B **60** 15063–73
[26] Shieh S and Duffy T S, 2002 *Phys. Rev. Lett*. **89** 255507
[27] Singh A K, Andrault D and Bouvier P 2012 *Phys. Earth Planet. Mater.* **208-209** 1–10
[28] Singh A K, Liermann H P, Saxena S K, Mao H-k and Usha Devi S 2006 *J. Phys.: Condens. Matter* **18** S969–78
[29] Duffy T S, Shen G, Shu J, Mao H K, Hemley, R J and Singh, A K 1999 *J. Appl. Phys.* **86** 6729–36
[30] Meng Y, Weidner D J and Fei Y 1993 *Geophy. Res. Lett.* **20** 1147–50
[31] Jing Q-M, Wu Q, Liu L, Bi Y, Zhang Y, Liu S-G and Xu J-A, 2012 *Cin. Phys.* B **21** 106201
[32] Brandes E A 1983 *Smithell's Metals Reference Book*, Butterworths London pp. 22–3
[33] Cubberly W H, Baker H, Benjamin D, Unterweisser P M, Kirkpatrick C W,Knoll V and Nieman K 1979 *Metal Handbook*, **2**, American Society for Metals, Metals Park, OH, USA
[34] Singh A K, Liermann H-P, Akahama Y and Kawamura H 2007 *J. Appl. Phys.* **101** 123526
[35] Singh A K, Jain A, Liermann H-P and Saxena S K 2010 *J. Phys. Chem. Solids* **71** 1088–93
[36] Singh A K, Jain A, Liermann H-P and Saxena S K 2006 *J. Phys. Chem. Solids* **67** 2197–202
[37] Singh A K, Liermann H-P, Akahama Y, S K Saxena and Menéndez-Proupin E 2008 *J. Appl. Phys.***103** 063524
[38] He D W and Duffy T S 2006 *Phys. Rev.* B **73** 134106
[39] Dieter G E 1988 *Mechanical Metallurgy – SI Metric Edition* (Singapore: McGraw-Hill) p. 520
[40] Hall E O 1951 *Proc. Phys. Soc. (London)* B **64** 747–53
[41] Petch N J 1953 *J. Iron Steel Inst.* **174** 25–8